NOTES AND CORRESPONDENCE

Synoptic-Scale Controls of Summer Precipitation in the Southeastern United States

Jeremy E. Diem

Department of Anthropology and Geography, Georgia State University, Atlanta, Georgia

(Manuscript received 15 October 2004, in final form 11 August 2005)

ABSTRACT

Past climatological research has not quantitatively defined the synoptic-scale circulation deviations responsible for anomalous summer-season precipitation totals in the southeastern United States. Therefore, the objectives of this research were to determine the synoptic-scale controls of wet and dry multiday periods during the summer within a portion of the southeastern United States as well as to assess the linkages between synoptic-scale circulation and multidecadal variations in precipitation characteristics for the study domain. Daily precipitation data from 30 stations for June, July, and August from 1953 to 2002 were converted into 13-day totals. Using standardized principal components analysis (PCA), the study domain was divided into three precipitation regions (i.e., South, Northwest, and Northeast). Wet and dry periods for each region were composed of the top 56 and bottom 56 thirteen-day periods. Composite circulation maps for 500 and 850 mb revealed the following: wet periods were generally associated with an upper-level trough over the interior southeastern United States coincident with strong lower-tropospheric flow into the Southeast from the Gulf of Mexico, and dry periods were characterized by ridges or anticyclones over the midwestern and southeastern United States coupled with weak lower-tropospheric flow. Many of the wet periods had surface fronts. Over the 50-yr period, increased precipitation was significantly correlated with increased occurrences of midtropospheric troughs over the study domain. Future research can benefit from the main finding of a strong impact of synoptic-scale circulation features on summer precipitation in the southeastern United States.

1. Introduction

The humid subtropical climate type, which has been characterized by the usual absence of summer droughts, exists on nearly every large landmass (Trewartha and Horn 1980). Most humid subtropical climates are located on the southeastern part of landmasses between the Tropics and ~40° latitude, and the largest expanses of the climate type exist in the southeastern United States, southeastern South America, and eastern China. Extensive urbanization has occurred in humid subtropical regions: the climate type is home to Tokyo, Japan; Buenos Aires, Argentina; and Beijing, China. Furthermore, with its warm and often wet summers, the humid subtropical climate type supports millions of hectares of agricultural lands. Consequently, enhanced knowledge of synoptic-scale controls of warm-season wet and dry periods is needed to better understand the potential impacts of climate on public welfare.

By controlling moisture transport into the continents as well as influencing the overall stability of the atmosphere, oceanic subtropical anticyclones greatly influence summer precipitation at most humid subtropical locales. The Bermuda high, the South Atlantic high, and the western Pacific high affect summer precipitation in the southeastern United States (e.g., Henderson and Vega 1996), southeastern South America (e.g., Diaz and Aceituno 2003), and eastern/southeastern China (e.g., Samel et al. 1999), respectively. The Bermuda high index (BHI) measures the slope of the sea level pressure gradient between Bermuda and New Orleans, Louisiana (Stahle and Cleaveland 1992); and positive BHI values typically indicate enhanced southerly moisture advection and reduced stability over the southeastern United States (Henderson and Vega 1996). For the 1946–88 period, Henderson and Vega

Corresponding author address: Dr. Jeremy E. Diem, Department of Anthropology and Geography, Georgia State University, Atlanta, GA 30303-3083.
E-mail: gegjed@langate.gsu.edu

© 2006 American Meteorological Society

Unauthenticated | Downloaded 05/15/25 03:30 PM UTC

(1996) reported a significant positive correlation between the BHI and summer precipitation totals within the southeastern United States. In contrast, over approximately the 1900–90 period, Keim (1997) did not find a significant correlation between the BHI and seasonal frequency of heavy rainfall events at locales proximate to the Gulf of Mexico and the Atlantic Ocean. Nevertheless, by only considering four weather stations that were not in the key southeastern states of Alabama, Georgia, and South Carolina, Keim (1997) disregarded most of the southeastern United States with the correlation analyses.

Midtropospheric troughing also can impact summer precipitation substantially in the southeastern United States. Using seasonal values of the Pacific–North American index (PNAI), whose large positive values indicate meridional flow over North America and large negative values indicate strong zonal flow over the continent, Henderson and Robinson (1994) and Henderson and Vega (1996) found a significant positive correlation between the PNAI and summer precipitation throughout the Southeast. In the southern Appalachian Mountains, even weak troughs can provide enough ascent and enable sufficient moisture transport to support thunderstorm development (Weisman 1990). Often associated with troughing are surface fronts: heavy thunderstorm activity in the lee of the southern Appalachian Mountains is caused frequently by frontal activity linked to an upper-level trough (Easterling 1991). Keim (1996) and Konrad (1997) also determined that most of the warm-season heavy precipitation events in the southeastern United States are associated with synoptic-scale disturbances (e.g., fronts). Moreover, Gamble and Meentemeyer (1997) found the most frequent ascent mechanism for summer flood events in the Southeast was a front with upper-air enhancement.

Although past climatological research has shown that changes in the synoptic-scale circulation significantly impacts warm-season precipitation in the southeastern United States, the research has not provided a quantitative assessment of circulation deviations responsible for extreme periods. The extreme periods can impact substantially seasonal precipitation totals. Therefore, the objectives of this research are 1) to determine the synoptic-scale controls of wet and dry multiday periods during the summer season within a portion of the southeastern United States, and 2) to assess the linkages between synoptic-scale circulation and multidecadal variations in precipitation characteristics for the study domain. The extended Atlanta, Georgia, metropolitan area is selected as the study domain, because, based on its geographical position, it represents well the southeastern United States and it contains daily pre-

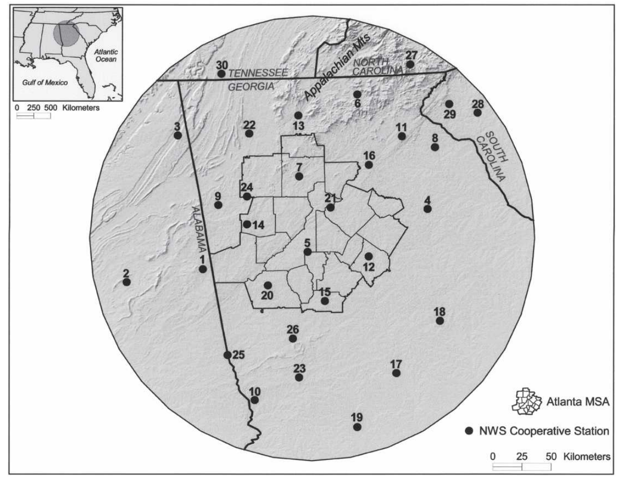

FIG. 1. Map of the study domain showing locations of the 30 precipitation stations as well as the boundary of the Atlanta metropolitan area. Numbers denote the precipitation stations; station names and associated information are available in Table 1.

cipitation data over a multidecadal period for a dense network of weather stations (Fig. 1).

2. Data

The study primarily required daily data from June, July, and August of 1953–2002. Therefore, daily precipitation totals, daily upper-level atmospheric data, daily weather maps, and daily tropical system data were acquired for that period. In addition, monthly sea level pressure (SLP) data were obtained.

Daily precipitation totals measured at 30 stations within 180 km of Atlanta were extracted from the TD3200 and TD3210 databases created by the National Climatic Data Center (NCDC; Fig. 1; Table 1). Since complete details of the precipitation data are provided in Diem and Mote (2005), only a summary is presented here. The 30 stations were spatially dispersed throughout the domain. Less than 0.5% (i.e., 649 out of 138 000) of the daily precipitation totals were missing; those missing values were estimated using an inverse distance weighting (IDW) scheme involving data from at least two nearby stations. IDW has been found to be just as accurate as other missing-value-estimation methods (Xia et al. 1999). While all morning-measured precipitation totals were moved to the previous day, nearly all precipitation totals measured in the afternoon/evening were assigned to the day on which the measurement was taken. It was assumed that precipitation totals measured at the Automated Surface Observation System (ASOS) tipping-bucket gauges were underestimates relative to precipitation totals at standard gauges.

Unauthenticated | Downloaded 05/15/25 03:30 PM UTC

Table 1. Characteristics of the 30 weather stations used in the study. Stations can be located in Fig. 1 using the numbers under "ID." "Coop ID" is the National Weather Service's Cooperative Station Network identification number for the station. "Percent missing" refers to the percent of days without valid daily precipitation totals.

ID	Station	State	Coop ID	Database	Percent missing	Lat (°)	Lon (°)
1	Hightower	AL	13842	TD3200	3.0	33.53	−85.40
2	Talladega	AL	18024	TD3200	0.2	33.44	−86.10
3	Valley Head	AL	18469	TD3200	0.1	34.56	−85.62
4	Athens	GA	90435	TD3210	0.1	33.95	−83.32
5	Atlanta Airport	GA	90451	TD3210	0.0	33.65	−84.43
6	Blairsville	GA	90969	TD3200	0.0	34.85	−83.94
7	Canton	GA	91585	TD3200	0.0	34.23	−84.50
8	Carnesville	GA	91619	TD3200	0.6	34.42	−83.23
9	Cedartown	GA	91732	TD3200	0.2	34.02	−85.25
10	Columbus	GA	92166	TD3210	0.7	32.52	−84.94
11	Cornelia	GA	92283	TD3200	0.1	34.52	−83.53
12	Covington	GA	92318	TD3200	3.4	33.60	−83.87
13	Ellijay	GA	93115	TD3200	0.7	34.70	−84.49
14	Embry	GA	93147	TD3200	0.0	33.87	−84.99
15	Experiment	GA	93271	TD3200	0.9	33.27	−84.28
16	Gainesville	GA	93621	TD3200	0.2	34.30	−83.85
17	Macon	GA	95443	TD3210	0.0	32.70	−83.65
18	Milledgeville	GA	95874	TD3200	1.5	33.09	−83.24
19	Montezuma	GA	95979	TD3200	0.1	32.29	−84.02
20	Newnan	GA	96335	TD3200	0.2	33.40	−84.80
21	Norcross	GA	96407	TD3200	0.0	33.99	−84.21
22	Resaca	GA	97430	TD3200	0.1	34.57	−84.95
23	Talbotton	GA	98535	TD3200	0.5	32.68	−84.54
24	Taylorsville	GA	98600	TD3200	0.2	34.08	−84.98
25	West Point	GA	99291	TD3200	1.0	32.87	−85.18
26	Woodbury	GA	99506	TD3200	0.3	32.98	−84.58
27	Coweeta	NC	312102	TD3200	0.0	35.07	−83.43
28	Clemson	SC	381770	TD3200	0.1	34.68	−82.82
29	Walhalla	SC	388887	TD3200	0.0	34.75	−83.08
30	Chattanooga	TN	401656	TD3210	0.0	35.03	−85.20

Therefore, ASOS-measured precipitation values were multiplied by 1.12 to adjust for the suspected reduced precipitation totals associated with the tipping-bucket gauge (see Diem and Mote 2005 for the explanation). Fortunately, tipping-bucket gauges measured less than 3% of the daily precipitation totals. The final precipitation database was serially complete for all 30 stations for the 50-yr period.

Daily atmospheric data for the entire period were extracted from the National Centers for Environmental Prediction–National Center for Atmospheric Research (NCEP–NCAR) reanalysis dataset (Kalnay et al. 1996) of the Climate Diagnostics Center (CDC) of the National Oceanic and Atmospheric Administration (NOAA) and the Cooperative Institute for Research in Environmental Sciences (CIRES) daily weather maps were provided by NOAA's Central Library Data Imaging Project, and tropical system tracks were provided by the National Weather Service's National Hurricane Center. The daily NCEP–NCAR data included the following: 850-mb geopotential heights, 850-mb wind direction, 850-mb wind speed, and 500-mb geopotential heights. Using the daily 500-mb surfaces, upper-level troughs and closed lows directly over or to the immediate west of the study domain were identified.

Additional data were obtained for the development of the BHI and the PNAI. Monthly SLP data needed for the BHI were obtained from the NCEP–NCAR reanalysis dataset (Kalnay et al. 1996) at grid points corresponding to Bermuda (32.33°N, 64.75°W) and New Orleans (29.95°N, 90.10°W). Standardized monthly SLP at New Orleans was subtracted from standardized monthly SLP at Bermuda (Stahle and Cleaveland 1992). Monthly PNAI values generated by the modified-pointwise method were provided by NOAA's Climate Prediction Center.

3. Methods

a. *Regionalization*

The domain was divided into precipitation regions to enable a more parsimonious examination of the circu-

Unauthenticated | Downloaded 05/15/25 03:30 PM UTC

lation controls of wet and dry periods. The delineation of precipitation regions ensures that findings apply to a region rather than a specific station; in addition, the pooling of data within a region helps minimize the impacts of station-specific discontinuities (Easterling and Peterson 1995).

The precipitation data were transformed in several ways. After removing 31 August from the database to produce a 91-day season, 13-day precipitation totals were calculated. Thirteen days was the smallest aggregate that had a nonzero mode frequency distribution. This resulted in a total of 350 observations for each station. Because the 13-day totals still were positively skewed, a square root transformation was used to produce approximately normal distributions.

The regionalization was based on an S-mode standardized principal components analysis (PCA; e.g., Richman and Lamb 1985; White et al. 1991; Comrie and Glenn 1998). To find stations that either switched regions over time or were not solidly within a region or both, separate regionalizations were performed for the following overlapping periods: 1953–82, 1963–92, and 1973–2002. Each input matrix consisted of 30 variables (i.e., stations) and 210 observations (i.e., 210 thirteen-day values). The use of a correlation matrix ensured that stations with similar temporal variations, as opposed to similar precipitation magnitudes, were grouped together; therefore, the correlation matrix facilitated compositing (i.e., stations in a particular region should have similar wet and dry periods). Results from two common component rotation techniques—orthogonal rotation (i.e., varimax) and oblique rotation (i.e., direct oblimin)—were compared, and the technique that produced the more physically justifiable regions was used. The maximum-loading rule was used to associate a station with a particular component (i.e., region). Histograms of rotated component loadings were examined for break points representing critical loadings values (i.e., a station is in a region if its loading is equal to or greater than the critical value). If the loading for a station was equal to or greater than the critical value, then that station was placed into the region for which it had a "significant" loading. All stations with loadings that did not exceed the critical value were deemed transitional stations; furthermore, stations that switched regions over time were also given the transitional status. Precipitation totals at the transitional stations were not used in the precipitation-to-circulation analyses.

b. *Precipitation-to-circulation analysis*

Composites were created to assess synoptic-scale controls of wet and dry periods in the regions. The transformed 13-day precipitation totals at each station were transformed further into standardized values (i.e., z scores); the standardization was specific to each station. The standardization reduced the likelihood of a 13-day period being classified as an extreme period based on an extreme value at a minority of the stations within a region. The mean of all station-specific z scores within each region was calculated. Thirteen-day periods with mean z scores more than one standard deviation above the mean were classified as wet periods, while periods with z scores more than one standard deviation below the mean were classified as dry periods.

Circulation patterns for the wet and dry composites were constructed, and those patterns were compared with mean summer-season patterns over the 1953–2002 period. Thus, 850- and 500-mb anomaly maps were created for wet and dry composites of each region. The anomaly maps were constructed to reveal spatial changes in circulation features.

Weather conditions for individual days within the wet periods were examined. Wet-period days with the largest precipitation totals within their 13-day periods also were selected, and the occurrence of troughs, tropical systems, and fronts on those days was noted. Troughs and closed lows were identified on daily 500-mb maps, fronts were identified through the examination of daily weather maps, and tropical system days were identified by examining annual maps of tropical system tracks. All days with a tropical system within a 350-km-radius circle centered on Atlanta were classified as tropical system days. Thus, even if only one station may have been affected by a tropical system, that day was classified as a tropical system day. Tropical system swath size was based on methods and results in Rodgers et al. (2001).

Interannual variations in the wet-period frequency, dry-period frequency, and summer precipitation were also assessed. Correlations between the above variables and troughing frequency, BHI, and PNAI were tested using the Spearman rank order test. This nonparametric test was used instead of parametric tests (e.g., Pearson product moment correlation), because some of the variables did not have normal, or near-normal, distributions. The chosen significance level was $\alpha = 0.05$ for the one-tailed tests.

4. Results and discussion

a. *Regionalization*

The PCA-based regionalization resulted in three regions for each 30-yr period. Each scree plot of eigenvalues indicated that three components should be retained and thus subjected to rotation. The cumulative

Unauthenticated | Downloaded 05/15/25 03:30 PM UTC

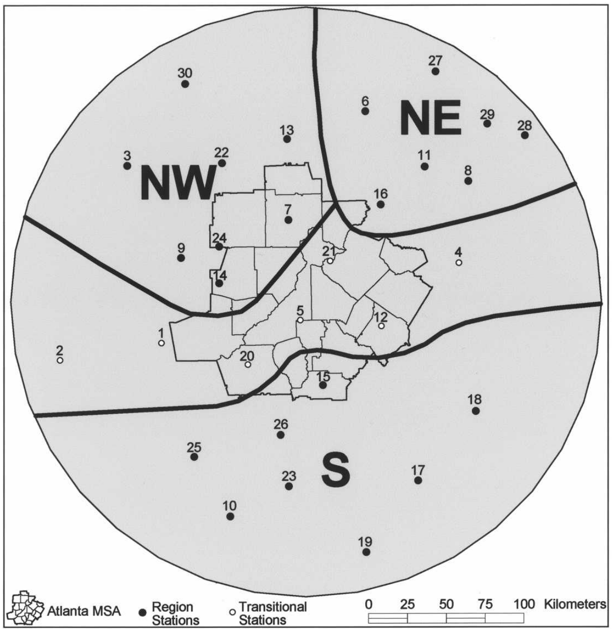

FIG. 2. The study region divided into the South (S), Northwest (NW), and Northeast (NE) summer-precipitation regions. A transitional zone extends longitudinally across the middle of the study domain. Also shown are the NWS cooperative stations within the study domain; refer to Table 1 for station names and associated information.

explained variance of the three components ranged from 62% to 64%. Component rotation using varimax and direct oblimin produced similar results for all three periods; however, regionalizations based on maximum varimax-derived loadings were more logical from both climatological and topographical perspectives. Therefore, the final regionalization was based on component loadings rotated with the varimax technique. Although stations were assigned initially to the component (i.e., region) on which the maximum loading existed, examinations of loadings for all three epochs indicated that the critical loading occurred near 0.58. Therefore, a station was assigned to a region if $\gamma \geq 0.58$. The final regionalization resulted in three regions (i.e., South, Northwest, and Northeast) containing 23 of the 30 stations (Fig. 2). The seven remaining stations (i.e., transitional stations) occupied an east–west swath across the study domain.

b. Precipitation-to-circulation analysis

Wet and dry periods for each region were composed of the top 56 and bottom 56 thirteen-day periods, respectively, based on mean z scores. The distributions of mean z scores for each region were normally distributed, thus the wet and dry periods had mean z scores greater than one standard deviation from the mean. Since composites were based on 13-day periods, the 728 days in a wet or dry composite were not the 728 wettest or driest days of the 4600 summer days from 1953 to 2002. The mean daily precipitation total for the wet periods (8.0 mm) was 10 times larger than the mean value for the dry periods (0.8 mm).

1) WET PERIODS

Wet periods for all three regions coincided with midtropospheric troughing to the west of the study domain as well as with substantial changes in lower-tropospheric circulation (Fig. 3). Large positive anomalies in 500- and 850-mb heights were located off the coast of and to the northeast of the northeastern United States, and large negative anomalies existed principally over the midwestern United States. The shifts in lower-tropospheric circulation features produced strong southwesterly flow into the Southeast, thereby enabling the advection of moisture from the Gulf of Mexico (Table 2). Midtropospheric troughs/closed lows were present on approximately 80% of the maximum-precipitation days, while fronts were present on approximately 40% of the maximum-precipitation days. Of the cumulative total of 168 wet periods, only two of the periods, both of which coincided with the passage of Tropical Depression Jerry in August 1995, did not receive any troughing-related precipitation.

2) DRY PERIODS

Dry periods for all three regions coincided with a displacement of midtropospheric troughing to the east of the study domain (Fig. 4). Compared to the wet-period anomaly centers, the dry-period anomaly centers were located in the same general locations but were opposite in sign. The study domain was almost always under an anticyclone or near the western limb of a trough. The high pressure over the midwestern and southeastern United States took the form of either continental anticyclones or the westward expansion of the Bermuda high or the merger of both anticyclones. Coupled with the increased pressure over the continent was decreased pressure over the western North Atlantic Ocean. As a result of the shifts in anticyclones, dry periods for all three regions had weak westerly–northwesterly 850-mb flow over the study domain (Table 2).

3) INTERANNUAL VARIATIONS IN WET-PERIOD FREQUENCY, DRY-PERIOD FREQUENCY, AND SEASONAL PRECIPITATION

From 1953 to 2002, the study domain had the following precipitation characteristics: wet summers throughout the 1960s and again in the early 1990s; and dry summers during the mid-1950s, from the mid-1970s to the mid-1980s, and in the late 1990s. Wet-period fre-

Unauthenticated | Downloaded 05/15/25 03:30 PM UTC

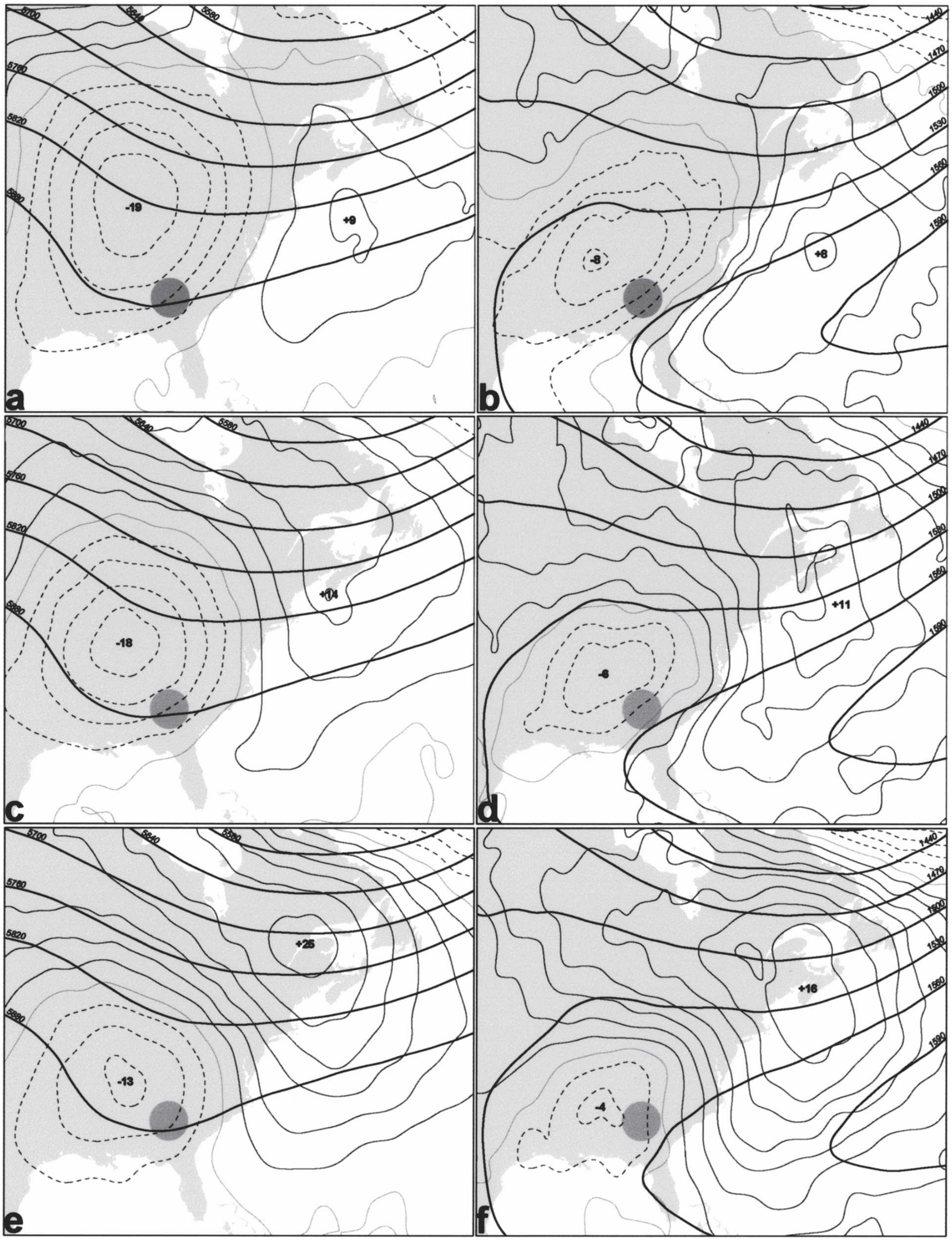

FIG. 3. Wet-period circulation patterns for the S at (a) 500 and (b) 850 mb, the NW (c) at 500 and (d) 850 mb, and the NE (e) at 500 and (f) 850 mb. Dark solid lines are the actual geopotential heights, while the thinner lines (solid and dashed) are anomalies. The signed numbers indicate the strength of the anomaly centers. Units are meters. The study domain is shown as a shaded circle.

quency peaked in the 1960s and especially in the early 1990s, while dry-period frequency had a major peak from the mid-1970s to the mid-1980s and another peak in the late 1990s (Fig. 5a). Tropical systems were infrequent, thus fewer than 10% of the wet periods were directly caused by precipitation from tropical systems. Seasonal precipitation, which was calculated as the mean value of all 30 stations in the study domain, was well connected to the difference in frequencies between wet and dry periods (Fig. 5b).

Unauthenticated | Downloaded 05/15/25 03:30 PM UTC

Table 2. Wind direction and wind speed at 850 mb on wet-period, dry-period, and typical days. Wind direction (WD) and wind speed (WS) are reported in ° and m s^{-1}, respectively.

Region	WD wet	WD dry	WD typical	WS wet	WS dry	WS typical
South	232	286	236	3.8	0.9	1.8
Northwest	238	284	249	3.1	1.0	2.1
Northeast	233	291	259	2.7	2.1	2.5

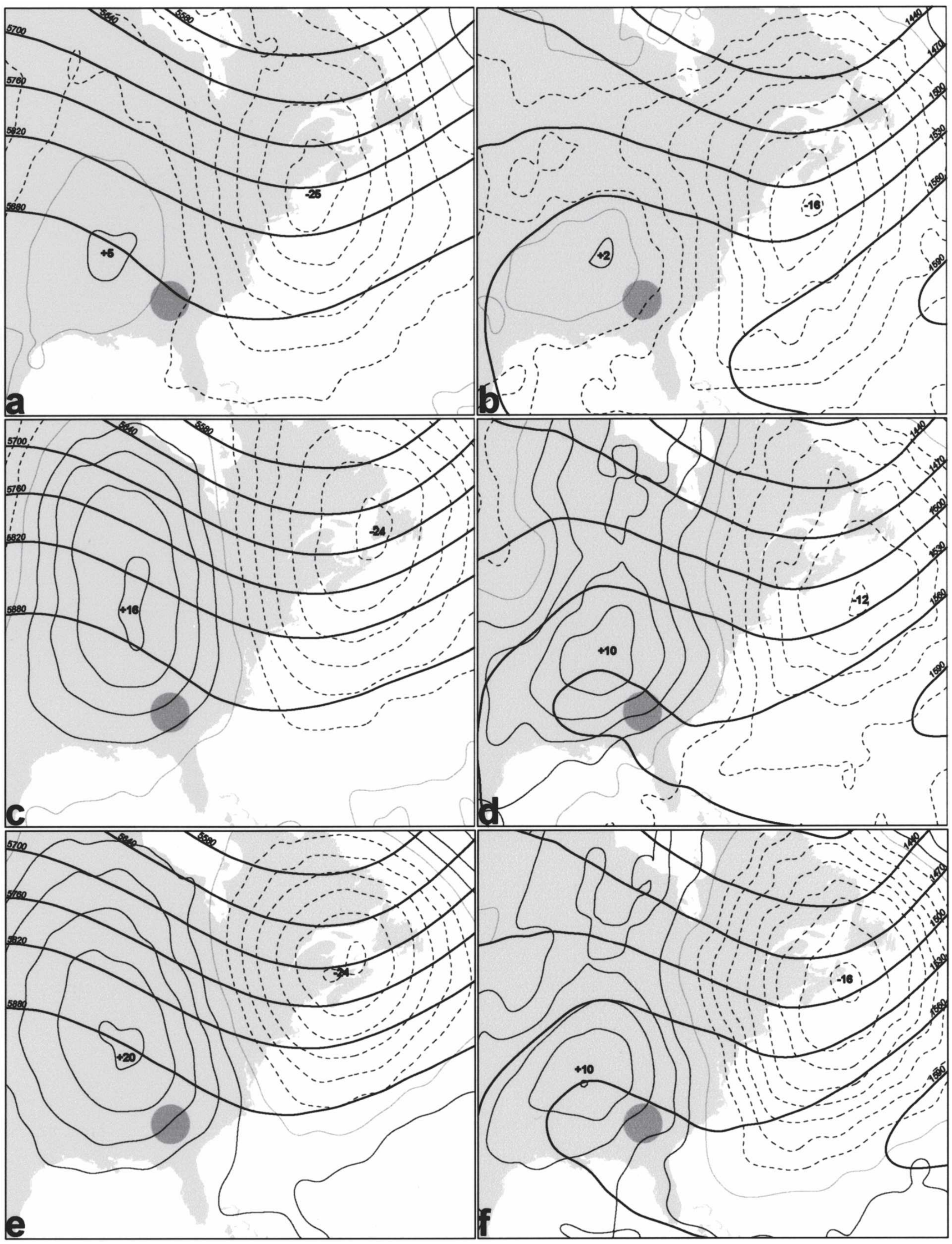

Fig. 4. Same as in Fig. 3, but for the dry-period circulation patterns.

Unauthenticated | Downloaded 05/15/25 03:30 PM UTC

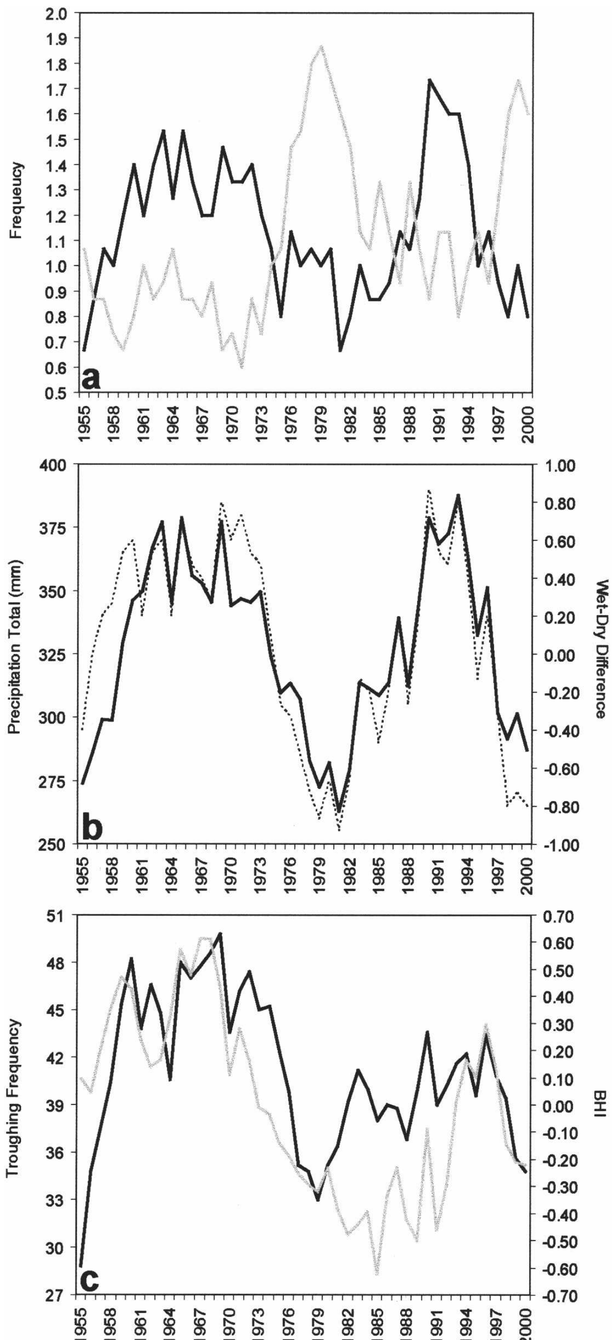

FIG. 5. Smoothed interannual variation in (a) wet-period frequency (solid black line) and dry-period frequency (solid gray line), (b) seasonal precipitation totals (solid black line) and wet-period frequency minus dry-period frequency (dashed line), and (c) seasonal troughing frequency (solid black line) and BHI (solid gray line). All precipitation-related values are the mean for the entire study domain. A 5-yr moving-mean filter was applied to the seasonal values.

Troughing frequency, rather than the BHI or the PNAI, was strongly correlated with wet-period frequency, dry-period frequency, and seasonal precipitation within the study domain (Table 3). All correlation coefficients for troughing frequency were statistically significant, and the largest coefficients occurred for seasonal precipitation totals. Increased (decreased) troughing was linked to more (less) precipitation. Although the BHI had mostly significant correlations, it was not correlated strongly with wet-period frequency. Finally, there was only one significant correlation between the PNAI and precipitation in the study domain, and all PNAI correlations were smaller than those for either troughing frequency or the BHI.

Multiyear highs and lows in wet- and dry-period frequency and seasonal precipitation were explained partially by changes in troughing frequency and the BHI (Fig. 5c). Concerning wet multiyear periods, the 1960s coincided with peaks in troughing frequency and the BHI, while the early 1990s did not have large values for troughing frequency or the BHI. Reduced troughing in 1993 was partially responsible for the smaller smoothed troughing frequency and BHI values in the early 1990s: the 1993 season had the second smallest troughing frequency and BHI values of the 50 summer seasons studied. The peak in dry-period frequency from the mid-1970s to the mid-1980s coincided with major depressions in troughing frequency, the BHI, or both. For the most part, wet summers (dry summers) were controlled by occurrences of substantial midtropospheric troughing (ridging) over the southeastern United States coupled with strengthened (weakened) lower-tropospheric circulation over the subtropical western North Atlantic Ocean and the Gulf of Mexico.

5. Conclusions

This research has examined synoptic-scale controls of summer precipitation within the extended Atlanta,

TABLE 3. Correlations between precipitation-related variables for the three regions and troughing frequency (TF), BHI, and PNAI. "Wet," "dry," and "season" refer to wet-period frequency, dry-period frequency, and seasonal precipitation, respectively.

Variable	TF	BHI	PNAI
S wet	+0.38*	+0.34*	+0.20
NW wet	+0.49*	+0.21	+0.02
NE wet	+0.44*	+0.16	−0.03
S dry	−0.36*	−0.46*	−0.24*
NW dry	−0.43*	−0.24*	−0.01
NE dry	−0.49*	−0.41*	−0.20
S season	+0.56*	+0.44*	+0.18
NW season	+0.62*	+0.19	−0.05
NE season	+0.60*	+0.36*	−0.01

* Significant ($\alpha = 0.05$) correlations.

Unauthenticated | Downloaded 05/15/25 03:30 PM UTC

Georgia, metropolitan area of the southeastern United States. Using 13-day precipitation totals from 1953 to 2002, a PCA-based regionalization resulted in three distinct regions (i.e., South, Northwest, and Northeast), with each region containing at least seven weather stations. Mean region-specific standardized precipitation totals were normally distributed, and a criterion of one standard deviation from the mean yielded 56 wet periods and 56 dry periods for each region. For all regions, wet periods were generally associated with an upper-level trough over the interior southeastern United States coincident with increased pressure off the eastern coast of the United States. Those circulation deviations resulted typically in increased moisture advection and increased frontal activity. Nearly opposite to the situation for wet periods, dry periods for all regions were characterized by ridges or anticyclones over the midwestern and southeastern United States coupled with decreased pressure off the eastern coast of the United States. Thus, precipitation-producing atmospheric processes were weakened.

Nonparametric correlation analyses—which involved extreme-period frequencies, seasonal precipitation totals, troughing frequency, the BHI, and the PNAI—and examinations of smoothed time series plots were used to examine linkages between synoptic-scale circulation and multidecadal variations in precipitation. Although correlations with the PNAI were mostly insignificant, strong correlations with troughing frequency and the BHI indicated that midtropospheric troughing (ridging) over the southeastern United States coupled with strengthened (weakened) lower-tropospheric circulation over the subtropical western North Atlantic Ocean and the Gulf of Mexico tended to cause wet summers (dry summers). Thus, synoptic-scale circulation impacts on wet and dry periods were transferable to larger temporal scales.

This research provides a foundation for continuing research on the impact of circulation variability on summer precipitation in the southeastern United States. It is vitally important to determine the causes of interannual variations in precipitation, and new circulation indices derived from height anomaly surfaces similar to those described in this paper could be used to explain precipitation variability during the second half of the twentieth century. Moreover, the new indices could be used in conjunction with existing circulation and teleconnection indices, such as the North Atlantic Oscillation (NAO) index, the Pacific decadal oscillation (PDO) index, the Southern Oscillation index (SOI), and the aforementioned BHI and PNAI.

REFERENCES

Comrie, A. C., and E. C. Glenn, 1998: Principal components-based regionalization of precipitation regimes across the southwest United States and northern Mexico, with an application to monsoon precipitation variability. *Climate Res.,* **10,** 201–215.

Diaz, A., and P. Aceituno, 2003: Atmospheric circulation anomalies during periods of enhanced and reduced convective cloudiness over Uruguay. *J. Climate,* **16,** 3171–3185.

Diem, J. E., and T. L. Mote, 2005: Inter-epochal changes in summer precipitation in the southeastern United States: Evidence of possible urban effects near Atlanta, Georgia. *J. Appl. Meteor.,* **44,** 717–730.

Easterling, D. R., 1991: Climatological patterns of thunderstorm activity in south-eastern USA. *Int. J. Climatol.,* **11,** 213–221.

——, and T. C. Peterson, 1995: A new method for detecting undocumented discontinuities in climatological time series. *Int. J. Climatol.,* **15,** 369–377.

Gamble, D. W., and V. G. Meentemeyer, 1997: A synoptic climatology of extreme unseasonable floods in the southeastern United States, 1950–1990. *Phys. Geogr.,* **18,** 496–524.

Henderson, K. G., and P. J. Robinson, 1994: Relationships between the Pacific/North American teleconnection patterns and precipitation events in the south-eastern USA. *Int. J. Climatol.,* **14,** 307–323.

——, and A. J. Vega, 1996: Regional precipitation variability in the southeastern United States. *Phys. Geogr.,* **17,** 93–112.

Kalnay, E., and Coauthors, 1996: The NCEP/NCAR 40-Year Reanalysis Project. *Bull. Amer. Meteor. Soc.,* **77,** 437–471.

Keim, B. D., 1996: Spatial, synoptic, and seasonal patterns of heavy rainfall in the southeastern United States. *Phys. Geogr.,* **17,** 313–328.

——, 1997: Preliminary analysis of the temporal patterns of heavy rainfall across the southeastern United States. *Prof. Geogr.,* **49,** 94–104.

Konrad, C. E., 1997: Synoptic-scale features associated with warm season heavy rainfall over the interior southeastern United States. *Wea. Forecasting,* **12,** 557–571.

Richman, M. B., and P. J. Lamb, 1985: Climatic pattern analysis of three- and seven-day summer rainfall in the central United States: Some methodological considerations and a regionalization. *J. Climate Appl. Meteor.,* **24,** 1325–1343.

Rodgers, E. B., R. F. Adler, and H. F. Pierce, 2001: Contribution of tropical cyclones to the North Atlantic climatological rainfall as observed from satellites. *J. Appl. Meteor.,* **40,** 1785–1800.

Samel, A. N., W.-C. Wang, and X.-Z. Liang, 1999: The monsoon rainband over China and relationships with the Eurasian circulation. *J. Climate,* **12,** 115–131.

Stahle, D. W., and M. K. Cleaveland, 1992: Reconstructing and analysis of spring rainfall over the southeastern U.S. for the past 1000 years. *Bull. Amer. Meteor. Soc.,* **73,** 1947–1961.

Trewartha, G. T., and L. H. Horn, 1980: *An Introduction to Climate*. McGraw-Hill, 416 pp.

Weisman, R. A., 1990: An observational study of warm season southern Appalachian lee troughs. Part I: Boundary layer circulation. *Mon. Wea. Rev.,* **118,** 950–962.

White, D., M. Richman, and B. Yarnal, 1991: Climate regionalization and rotation of principal components. *Int. J. Climatol.,* **11,** 1–25.

Xia, Y., P. Fabian, A. Stohl, and M. Winterhalter, 1999: Forest climatology: Estimation of missing values for Bavaria, Germany. *Agric. For. Meteor.,* **96,** 131–144.

Unauthenticated | Downloaded 05/15/25 03:30 PM UTC